



Published in final edited form as:

Dev Dyn. 2020 January ; 249(1): 125–140. doi:10.1002/dvdy.1119.

The Development of the Trunk Neural Crest in the Turtle *Trachemys scripta*.

Sophia Goldberg*, Akshaya Venkatesh*, Jocelyn Martinez*, Catherine Dombroski, Jessica Abesamis, Catherine Campbell, Mialishia Mccalipp, Maria Elena de Bellard[§]

California State University Northridge, Biology Dept., MC 8303. 18111 Nordhoff Street. Northridge, CA 91330

Abstract

Background: The neural crest is a group of multipotent cells that give rise to a wide variety of cells, especially portion of the peripheral nervous system. Neural crest cells show evolutionary conserved fate restrictions based on their axial level of origin: cranial, vagal, trunk and sacral. While much is known about these cells in mammals, birds, amphibians, and fish, relatively little is known in other types of amniotes such as snakes, lizards and turtles. We attempt here to provide a more detailed description of the early phase of trunk NCC development in turtle embryos.

Results: In this study, we show, for the first time, migrating trunk NCC in the pharyngula embryo of *Trachemys scripta* by vital-labeling the NCC with DiI and through immunofluorescence. We found that **A)** tNCC form a line along the sides of the trunk NT. **B)** The presence of late migrating tNCC on the medial portion of the somite. **C)** The presence of lateral mesodermal migrating tNCC in pharyngula embryos. **D)** That turtle embryos have large/thick peripheral nerves.

Conclusions: The similarities and differences in trunk NCC migration and early PNS development that we observe across sauropsids (birds, snake, gecko and turtle) suggests that these species evolved some distinct NCC pathways.

Keywords

turtle; neural crest; cell migration; HNK1; Sox10; peripheral nervous system; dorsal root ganglia

Introduction

The chordate peripheral nervous system originates largely from a group of multipotent stem cells known as the neural crest, which emerges after an epithelial-to-mesenchymal transition from the dorsal neural tube shortly after neural tube closure. After migrating rapidly throughout the developing embryo, these cells give rise to a wide variety of neuronal and glial derivatives in the peripheral nervous system (PNS), as well as parts of the head skeleton, melanocytes and endocrine organs (Clay and Halloran, 2010; Bronner and LeDouarin, 2012; Kague et al., 2012; Vega-Lopez et al., 2017). In anamniote vertebrates like

[§]Corresponding author. Telephone: 818-677-6470, FAX: 818-677-2034, maria.debellard@csun.edu.

*These authors contribute equally to the manuscript.

sharks and teleosts, NCC give rise to accompanying glial cells of electrosensory organs (Chien and Piotrowski, 2002) and fin mesenchyme (Smith et al., 1994; Hall, 2009; Gillis et al., 2017). Due to the NCC's versatility in giving rise to a wide range of derivatives, its evolution has resulted in major breakthroughs like the mammalian head and face, a sophisticated peripheral sensory nervous system and regenerating peripheral glia (Glenn Northcutt, 2005; Kastrić et al., 2019).

The neural crest in amniotes is commonly divided, based on their anterior to posterior origin, into specific cranial, vagal, trunk, and sacral crests (Le Douarin and Dupin, 2018). These axial populations express different cell potentials in amniotes. The cranial neural crest cells are the most versatile population as they can give rise to melanocytes, PNS cells, cranial and facial structures, corneal keratinocytes, and even olfactory glia (Santagati and Rijli, 2003; Baker, 2005; Barraud et al., 2010). Vagal NCC give rise to autonomic neurons as well as the enteric nervous system (Dupin et al., 2006; Simkin et al., 2019). However, the trunk neural crest cells (tNCC) have a more restricted potential, giving rise to sensory neurons, glial cells, supra-adrenal, melanocytes, and smooth muscle cells (Trentin et al., 2004; Creuzet et al., 2005; Baggiolini et al., 2015). Thus, tNCC in amniotes are a more restricted group of stem cells than cranial NCC.

Neural crest evolution however, is not only fascinating from the cranial point of view (Horie et al., 2018; Kuratani et al., 2018). They themselves have a right to be studied as a uniquely evolved population. Looking at tNCC across evolution, from the first organisms that have a defined tNCC, the anamniote chondrichthyans, through amniotes, there is one key element that co-evolves with peripheral cells: body shape differences. Because the sensory innervation of a water living organism has different constraints and adaptations than a terrestrial one. Moreover, a terrestrial organism with a thickened shell that protects its organs will need a different sensory system than one whose skin is more delicate. In other words, tNCC have to adapt/evolve along chordate evolution changes as much as cranial NCC do. This can be highlighted by the fact that in amphibians, trunk NCC follow a dorsal pathway into the fin and a ventral pathway between the neural tube and the caudal portion of the somite (Collazo et al., 1993). In zebrafish, tNCC numbers are small and these cells predominantly migrate between the neural tube and somites as in amphibians as well as in medial portion of somites (Sadaghiani and Vielkind, 1990; Eisen and Weston, 1993; Halloran, 2010; Theveneau and Mayor, 2012; Richardson et al., 2016). However, in amniotes like chicken and mouse, there are a large number of tNCC and these follow two main courses shortly after emigrating from the neural tube: a ventromedial pathway through the rostral part of somites, and a dorsolateral pathway between somites and ectoderm (Serbedzija et al., 1989; Kulesa and Gammill, 2010; Giovannone et al., 2015). Thus, while these cells give rise to mostly the same structures in amniotes and anamniotes, their migratory pathways and likely their numbers are quite different.

Perhaps the most interesting among all the vertebrates is the reptile NCC which are unique among vertebrates given their varied body structures. The majority of terrestrial reptiles have between 23 and 26 presacral vertebrae, while snakes have a variable number that can reach 300 vertebra (Williston and Gregory, 1925). Reptiles also have the unique feature of hardened scales covering their bodies, as well as the capacity to change skin color. Thus,

they pose special challenges to the PNS pathway as well as associated melanocytic pathway elucidation (Kundrat, 2008; Reyes et al., 2010; Cebra-Thomas et al., 2013; Rice et al., 2017). All these features point to the uniqueness of reptile NCC and its derivatives.

Turtle NCC has been studied using HNK1 as a marker. In 1994, Hou and Takeichi looked at a range of embryos (from stage 11-14) in the soft shell turtle (*Trionyx sinensis*) and observed that the trunk NCC had two pathways: dorsolateral with very few cells and what is now referred as ventro-medial (Hou and Takeuchi, 1994). More importantly, Cebra-Thomas, Gilbert and colleagues identified a large population of late emerging tNCC cells in the carapacial dermis of *Trachemys scripta* turtle embryos (stage 17) that were positive for HNK1, p75 and FoxD3 (Cebra-Thomas et al., 2007; Cebra-Thomas et al., 2013). While these studies provide unique discoveries describing turtle NCC migration, we still lack an overall knowledge of turtle tNCC. We aim to extend/improve on that excellent past work and provide a more detailed embryological description of turtle trunk NCC migration.

To better understand the evolution of NCC in more detail, we examined the neural crest in the turtle *Trachemys scripta* (Red-eared slider) using vital dye labeling and fluorescent immunostaining. We found that trunk neural crest migration in turtle followed the overall patterns observed in snake, birds, and mammals, with most first waves of migrating trunk NCC traveling through the rostral portion of the somites; however, there is a later group that migrates through the middle portion. Interestingly, we also found tNCC from pharyngula stages embryos migrating through mesoderm, suggesting these first waves of tNCC may be able to contribute to plastron and carapace. Finally, we observed that the turtle spinal nerves are thick and larger than that of the gecko.

Results

Turtle trunk NCC shows unique patterns of migration

In order to expand on what we already know about the migration of trunk NCC (tNCC) in the turtle, we injected embryos ranging from stages 7 to 13 (Tokita and Kuratani, 2001; Cordero and Janzen, 2014) with DiI inside their developing neural tubes (NT) and incubated them for 4-24 hrs (HPI: hours post injection) before fixation. We could not get embryos at stages 7-9 to survive DiI injection past 8 hrs under our culture conditions, thus our relevant data (24HPI) is restricted to embryos older than stage 9. Our sole stage 8 injected embryo survivor (8HPI) showed few delaminated trunk NCC outside the NT (Fig.1A). However, older embryos (past stages 9) survived the DiI injection better and we were able to incubate them for 24 hours (24HPI). The surviving DiI embryos (we had a 50% survival rate) provided some new findings on tNCC migration patterns as well as conserved ones. As expected, we regularly observed newly delaminated tNCC on top of neural tube (NT) in different embryonic stages post DiI injection (green arrows in Fig.1B, C, E). Overall, the pattern of tNCC migration is similar to the chicken (Giovannone et al., 2015). But, we observed some unique aspects in turtle tNCC migration.

Our **first** new finding on turtle tNCC migration was in embryos from stage 10 to st.13: a line of DiI cells along the sides of the trunk NT (white arrows in Fig.1F, G). Our **second** finding on turtle tNCC was in several of the DiI injected embryos: tNCC migrating through the

middle portion of the somite, not rostral or caudal (red arrows in Fig.1D, J and in more detail in Fig.2). A prominent observation was the presence of coalesced DRG and sympathetic chain posterior to hindlimb in stage 11 embryos (Fig.1D, F, J and Fig.3). As we had observed in the past for a snake, we saw that some DiI-cells were migrating between somites (arrows in Fig.1H).

The above observations were confirmed by using HNK1 staining in varied stages of turtle embryos (Fig.3 and Fig.4). We stained wholemount embryos with HNK1 since it is a well-known NCC marker for chicken as well as reptiles like turtles, snakes and crocodile (Loring and Erickson, 1987; Del Barrio and Nieto, 2004; Cebra-Thomas et al., 2007; Kundrat, 2008; Reyes et al., 2010). While HNK1 has been used in pharyngula stage turtle embryo (Hou and Takeuchi, 1994), there has been no extensive HNK1 labeling of wholemount turtle embryos during the initial stage of NCC migration (st.8-11) and immediately after (st. 12-14). Rice et al. published wholemount HNK1 staining of Cordero St.11 onwards, but our study examines HNK1 expression in more detail (Rice et al., 2017). We carried out a systematic labeling of turtle embryos with HNK1 to look at the migratory pattern of tNCC. Tail ends and midtrunk wholemount with HNK1 showed the line of tNCC along the trunk (white arrowheads in Fig.3D and Fig.4C–F). We were also able to observe tNCC migrating through the middle of somites (white arrows in Fig.3C–E, G and Fig.4E–F). In several embryos stained with HNK1, we observed that a portion of lateral mesoderm had HNK1-cells (red arrows in Fig.3B–D, H), as well as staining between the main tNCC migratory streams (red arrowheads in Fig.3H).

A stage 10 embryo labeled in wholemount with HNK1 showed that at more posterior trunk levels there were many migrating tNCC on the anterior portion of the somites, while at the more rostral levels there was clear evidence of the DRG condensation (Fig.4). In this head-to-tail wholemount we observed the classic pattern of segmentally migrating tNCC along the trunk between limbs (Fig.4B–F). But interestingly, we also observed a bright region of HNK1-positive cells migrating down into lateral mesoderm of the trunk (red arrows in Fig.4D–E, I). This mesodermally migrating group of tNCC make our *third* novel finding for turtle tNCC. Sections through these embryos showed that turtle NCC migrate along the ventromedial pathway in very large numbers in a clearly segmental manner and with development starting at more rostral levels and progressing caudally (Fig.4G–H). We were able to corroborate that the mesodermally located HNK1 cells between the two limb buds were not cells along the standard ventro-medial pathway, but were cells migrating more lateral to the aorta, into a tissue extension (arrow in Fig.4I and data not shown). Sections at the forelimb level showed HNK1 cells condensing as DRGs as well as some cells migrating under the ectoderm, which are likely melanoblasts (arrowhead in Fig.4G–H). Sections close to forelimb also showed a group of HNK1 cells inside the developing gut (white arrow in Fig.4H). A more caudal section showed a number of delaminating and migrating tNCC (arrowhead in Fig.4I) as well the unique tNCC in lateral mesoderm (red arrows in Fig.4I and data not shown).

A stage 11 DiI-injected embryo (24HPI) triple-labeled with HNK1 and Tuj1 (beta III tubulin neuronal marker in vertebrates) highlighted the observations described above (Fig.5). Section through st.14-15 embryos showed tNCC along traditional destinations of the DRG

and sympathetic ganglia cells, which were consistently positive for DiI and HNK1. In these sections we found our *fourth* new finding: very prominent, thick peripheral nerves. We observed HNK1 cells along the nerve, these are likely Schwann cell precursors (arrowhead in Fig.5D). We also observed DiI/HNK1 in mesonephric tissue (arrow in Fig.5B). Interestingly, Tuj1 did not label most of the HNK1-positive cells in the DRG, suggesting these cells have not fully differentiated yet (Fig.5C, G), but it did label consistently the ectoderm of the turtle embryo (Fig.5).

As development progressed, we could observe DiI cells as well as HNK1-positive in more embryonic tissues. Sections through some more DiI and HNK1 labeled embryos corroborated wholemount images that turtle DiI and HNK1-labeled tNCC followed the regular ventro-medial pathway (Fig.6). A stage 12 embryo labeled with DiI highlighted a large number of DiI migrated tNCC in the sympathetic ganglia (arrow in Fig.6A). In this same section it can be observed that tNCC are still delaminating (arrowhead in Fig.6A). We also observed a few, scattered labeled cells under the ectoderm, presumably melanoblasts (red arrowhead in Fig.6A). A younger embryo (stage 10) showed NCC in the developing gut (arrow in Fig.6C) plus newly delaminated tNCC hovering above the NT in larger volumes (Fig.6C, D and inserts). Since the work by Gilbert and colleagues showed that late tNCC will still delaminate and migrate (Cebra-Thomas et al., 2007) we injected an older embryo (stage 13) with DiI, this embryo had already well formed DRG. We observed clear presence of a late migrating group of DiI cells above the NT (arrow in Fig.6B) as found by Cebra-Thomas and co-workers.

Turtle PNS develops while tNCC is still migrating

The observation from previous figures 2–4 suggested a prominent condensation of the DRGs and larger than usual spinal nerves in turtle embryos. Sections through older turtle embryos supported the view that their peripheral spinal nerves were especially large (Fig.7). HNK1 and/or Tuj1 staining showed: **A**) that nerves were thicker than what is observed in somewhat-comparable chicken and gecko embryos (red arrows in Fig.7D, E). We measured the width of spinal nerves from section and wholemount 20 μ m below the DRG and found that consistently, turtle nerves were thicker than comparable gecko embryos (turtle 18 μ m, gecko 13 μ m, $p < 0.00001$, $N = 10$ turtle embryos, 5 gecko embryos). **B**) That there were HNK1-positive cells condensed in lateral mesenchyme (white arrow in Fig.5B, white arrows in Fig.7A, E). In older turtle embryos (st.15, before carapace is visible) we could see a Tuj1 labeled DRG (white arrowhead in Fig.7F) and a prominent thick spinal nerve (white arrow Fig.7G).

Because little is known about the progress of development of the PNS in turtles, we took advantage of the fact that turtle neurons were strongly labeled with Tuj1 antibody to do wholemount immunostaining of turtle embryos (Fig.8). For comparison purposes we generated composite stitched images of stage 10 embryos labeled either with HNK1 (Fig.8B) or Tuj1 (Fig.8A, C). At more rostral trunk levels (forelimb) embryos showed very thin spinal nerves (red arrows in Fig.8A, C), but as development progressed these nerves became longer and thicker, with DRG enlarging as well (white arrows in Fig.8A–C).

Higher magnification images of stage 13 embryos at the tail level labeled with Tuj1 highlighted this observation: at more caudal levels past the hindlimb, spinal nerves were thinner, but at more rostral levels the DRG were noticeably larger than posterior ones and the nerves were thicker with many peripheral branches (Fig.8D–G). Stained embryos also showed staining in-between the DRGs, likely sympathetic ganglia (arrow in Fig.8D, F–G). Sections through these embryos showed the progression of the DRG and spinal nerves development along the rostro-caudal axis (Fig.8F and data not shown). There appears to be ventral staining with Tuj1 (white arrowhead in Fig 8C), however these Tuj1-positive cells are different from the lateral mesoderm labeling we observed in DiI and HNK1-labeled embryos; these cells are ventral to the dorsal aorta (data not shown). We are not sure about the physiological meaning of this staining. We had noticed that some ectodermal cells express the anti-beta-III-tubulin (aka Tuj1 epitope) in the turtle, as well as gecko and amphibians (data not shown). Dr. Crystal Rogers has a manuscript under review showing that some ectodermal, possible NCC express TuJ1 as well (personal communication).

Pharyngula trunk Neural Crest likely contributes to Carapace and Plastron in the Turtle

Seminal work from the labs of Gilbert and Cebra-Thomas had demonstrated the existence of a late emigrating trunk NCC contributing to both carapace and plastron formation (Gilbert et al., 2007). Our earlier turtle embryos injected with DiI and/or labeled with HNK1 (as well as in situ with cSox10, data not shown) showed the presence of a delaminating tNCC population in earlier embryos along the flanks for plastron and dorsal portion for carapace (Fig.1–4). Therefore, we further examined our pharyngula turtle embryos in more detail for this phenomenon.

We observed that in stage 10-12 DiI embryos there were cells migrating into the lateral mesodermal tissue, this DiI location is a new observation, neither chicken or mouse embryos have tNCC in these locations (white arrows in Fig.9C). These DiI-positive lateral mesodermal ridge cells can also be seen in Fig.4 labeled with HNK1. In slightly older embryos (between stages 12-13), we observed HNK1-positive cells migrating laterally (arrows in Fig.9A–B, D–G). We noticed the presence of HNK1-positive cells between the DRGs that had been missed previously but which upon closer examination clearly belonged to scattered cells migrating along a different pathway from the ventro-medial one (Fig.9D, and magnifying inset in F–G).

Turtle PNS comparison with other reptiles

Our lab has been working with tNCC from other reptile embryos mostly using HNK1 to label these cells. Since we noticed some differences in the pattern from HNK1 staining, we wanted to do an overall appraisal of tNCC and the PNS amongst sauropsids (reptiles and aves). Here we stained trunk regions between limbs from chicken (*Gallus gallus*), gecko (*Gekko gekko*) and mid-body of snake (*Lampropeltis californiae*) embryos at somewhat comparable trunk stages (branchial arches not fused and having limb buds only in the case of chicken, turtle and gecko embryos). Specifically we wanted to look at tNCC during: A) first wave of delaminated cells, B) peak of migrating tNCC, and C) beginning of the DRG and peripheral nerves condensation. The first noticeable feature from this sauropsids comparison was that they all have very prominent DRG and spinal nerves (white arrows in

Fig.10C, F, I, L for spinal nerves). The second was the expected presence of a consistent ratio of space between the DRGs in all these sauropsids. In other words, DRG spacing at the neck level was equal than at the tail level. The third noticeable observation was that while segmented migration was well defined in all these species, the chicken and turtle show much larger volumes of migrating trunk tNCC (Fig.10B, D–E compared with 10G–H, J–K). The fifth and last observation from this comparison across sauropsids was that the first wave of delaminated tNCC in the turtle, Gecko and snake are very similar: the scattered cells (red arrows in Fig.10A, G, J) are more abundant than in chicken embryos (Fig.10D).

Discussion

In the present study, we provide an overall study of trunk NCC migration and its contribution to tissues in a turtle, the Red-eared slider *Trachemys scripta*. We examined early PNS development by live cell labeling with DiI and by using neural markers (HNK1, Tuj1). We found that tNCC in the red slider turtle are a) exhibiting same migratory patterns to the ones described for chicken; b) show unique migratory patterns unlike the known pathways in most amniotes, and c) the presence of pharyngula stage migrating trunk neural crest into lateral mesodermal tissue presents an intriguing possibility that it may contribute to the pool of carapace and plastron forming cells.

Unique aspects of the migration of turtle tNCC

Neural crest migration has been studied by using DiI and HNK1 in non-avian reptiles, including crocodile and turtle (Hou and Takeuchi, 1994; Kundrat, 2008), and just recently chameleon (Diaz et al., 2019). Hou and Takeuchi found that the migratory pattern of cranial and trunk neural crest in turtles followed more the paths reported for birds than for teleosts or *Xenopus*. In our present, more detailed study, we expand and supplement the findings of Hou and Takeuchi by studying a larger set of turtle embryos with DiI, HNK1 and Tuj1. We found that tNCC while following essentially the same migratory pathways as described for other reptiles and amniotes (Hou and Takeuchi, 1994; Dupin et al., 1998; Trainor, 2005), it presented unique migratory pathways not observed in other amniotes. These data suggest that while some core trunk migratory pathways are heavily conserved across all amniotes, the turtle has unique neural crest migratory pathways.

Here we observed **first**, that tNCC form a line along the sides of the trunk NT. **Second**, the presence of late migrating tNCC on the medial portion of the somite. **Third**, the presence of migrating tNCC that appears to be reaching the lateral mesoderm. **Fourth**, we showed that turtle embryos have large/thick peripheral nerves.

It is known that NCC move so rapidly that within 8 h after delamination they have reached most of their destinations in the avian and mouse embryos (Kulesa and Fraser, 2000; Kasemeier-Kulesa et al., 2005; Rogers et al., 2012). In our study, we incubated the embryos after labeling the neural tube with DiI for 8, 12 and 24 h, and found that after these time periods, large numbers of cells have reached the same locations as in other vertebrates including the dorsal aorta, mesonephros, cranial ganglia, melanocyte precursors and developing gut. In contrast to our past snake findings, we observed a large number of DiI labeled NCC (and HNK1) in the developing gut, showing that we were able to label vagal

NCC. It also shows that turtle NCC contribution to the enteric NS is as abundant as in other reported sauropsids (Le Douarin and Teillet, 1973; Reyes et al., 2010; Simkin et al., 2019).

While no inter-somitic migration has been reported in reptiles except for snake (Hou and Takeuchi, 1994; Reyes et al., 2010), we observed a number of inter-somitic migrating cells, though it seems to be a late event compared with the snake, chicken or mouse (Serbedzija et al., 1989; Serbedzija et al., 1992; Reyes et al., 2010). These findings suggest, as we have proposed in the past, that heavy utilization of the inter-somitic pathway by late-migrating NCC may be a derived feature of reptiles (Reyes et al., 2010). More detailed studies of trunk neural crest migration in other reptiles will be needed to determine which scenario was more likely. It will be interesting to determine whether non-avian reptile trunk neural crest migration is influenced by somatic repulsive factors in these early squamates, because NCC will migrate along the inter-somitic space in *Neuropilin 1* and *2* mutant mice (Schwarz et al., 2009).

We also observed a sizeable proportion of trunk NCC in the mesonephric region by using *DiI* and *HNK1* labeling as we observed in the snake. We found tNCC that migrated beyond the sympathetic ganglia region towards the mesonephroi. These cells do not correspond to those reported previously around the aorta (Serbedzija et al., 1989). While mesonephroi in birds are derived from mesodermal tissues, it has been suggested that snake mesonephroi could be partly neural crest derived (Gabe, 1970; Rupik, 2002). The present study supports such a possibility for turtles. Our results showed large amounts of *DiI* and *HNK1* labeled cells among the developing tubules, and that the shape of these labeled cells in older embryos is more epithelial than chromaffin cells (Fig.4D, 7I). Therefore, trunk neural crest appears to give rise to the adrenal chromaffin cells, and may contribute to portions of the developing kidney in the turtle.

Recently, studies have been highlighting the migratory behavior of NCC as collective or following contact inhibition of locomotion, as determined by a trailblazing group of cells (Schumacher et al., 2016; Szabo et al., 2016; McLennan et al., 2017). Although we observed this behavior in both fixed embryos and cultures of turtle NCC (data not shown), we also found several important concurrent results. **A)** Newly delaminated tNCC in turtle, gecko, snake and chameleon (Diaz et al., 2019) look more scattered and smaller in numbers in contrast to what has been observed in the chicken and mouse (see Fig.8) (Giovannone et al., 2015). **B)** This is followed by a second, much larger ventro-medial wave of tNCC that seemed to follow a more “collective” migratory pattern that is conserved across amniotes. **C)** Finally, we observed also another set of cells apparently “detached/separated” from this previous wave that migrates through the mesoderm. These cells likely contribute to the formation of the plastron.

Pharyngula trunk NCC may Contribute to Carapace and Plastron in the Turtle

In 2007, Cebra-Thomas and Gilbert showed that a good portion of the turtle plastron is derived from late delaminating NCC using *DiI* (Cebra-Thomas et al., 2007). However, they did not determine whether the early delaminating tNCC could also contribute to the carapace and plastron of turtles. Here we present strong evidence of such hypothesis. We show that our labeled turtle embryos, starting from pharyngula stages 11 through 15, show *DiI*, *Sox10*

and HNK-positive cells along the mesodermal tissue, the presence of these migrating tNCC presents an intriguing possibility that it may contribute to the pool of carapace and plastron forming cells.

Our most convincing data is the observation of a ventral band of HNK1 staining cells and the existence of migratory streams between the DRGs. While these are observations, not a demonstration that these are a ‘pool of shell forming cells’, it is along the lines of what has been shown for older tNCC and suggested for tNCC (Rice et al., 2016). What is even more relevant is that snakes also contain a ventral band of DiI/HNK1 cells (Fig.7A and 8E in (Reyes et al., 2010)) as well as chameleons (HNK1 in Fig.3G of (Diaz et al., 2019)).

In light of these findings, we would like to speculate that the tNCCs migrating in-between the DRGs and through mesodermal regions represent tNCCs with osteogenic capacity that will initiate plastron formation in the turtle and the scales of snakes. While trunk NCCs have not been shown to form skeletal elements in other amniotes besides turtles, several studies have shown that at least some trunk NCC can be induced to form bone experimentally *in vivo* (Graveson et al., 1997) and *in vitro* (McGonnell and Graham, 2002; Abzhanov et al., 2003; Ido and Ito, 2006). A more recent study showed that even mouse trunk NCC can give rise to chondrogenic cells without trying to re-program them (Replogle et al., 2018). This could indicate that the turtle tNCCs (and in other reptiles as well) are more like cranial NCCs from the start, and that a portion migrates into the presumptive plastron region while others differentiate along traditional trunk pathways into neurons, glia and melanocytes.

Turtle PNS development comparison with other reptiles

In addition to differences in the migration of late-emerging NCC, between snake and other amniotes, HNK1/Tuj1 staining revealed a noticeable difference in the shape of dorsal root ganglia (DRGs) across reptiles. We show that the shapes of embryonic DRG in turtle, chicken, gecko and snake are striking; turtles are large and oval compared with the smaller and spindle-shaped DRGs of snakes and geckos. Such differences in shape despite the initial conserved wave of migrating tNCC strongly suggests that the PNS in these sauropods goes through further developmental changes (further precursor cell division and/or pruning) as already shown for mouse and chicken (Levi-Montalcini and Booker, 1960).

Pertaining to the phylogeny of turtles, Brunneau and colleagues put forward the hypothesis of a convergence between warm- and cold-blooded organisms (Koshiba-Takeuchi et al., 2009). They link turtles closer to Archosauria based on heart structure and the evolution of a more active lifestyle. We would like to add to this hypothesis, that the large peripheral nervous system in turtles (larger number of migrating tNCC and larger spinal nerves) is more comparable to birds and mammals than to snakes; placing them closer to recent synapsids than to more ancient squamates. Thus, the characteristics of the turtle NCC was positioned between that of past and more recent evolutionary changes.

Recent phylogenetic studies using miRNA sequencing or available genomes have proposed new evolutionary branching among reptiles. For example, Field and coworkers using miRNA place turtles at more ancient branches than snakes and lizards (Field et al., 2014). However, Milinkovitch and colleagues, using transcriptomic from several reptiles, places

avians as the sister group to turtles and crocodile (Tzika et al., 2011). Additionally, the study of Zhang and co-workers used a larger and more comprehensive multilocus data set combining 22 nuclear genes and one mitochondrial fragment to provide a better, more encompassing look at turtle evolution and the separation among reptiles (Shen et al., 2011). Their final phylogeny of tetrapod evolution places the turtle separating at 257 mya from archosauria, and show strong supporting analysis that turtles are the sister group of Archosauria (birds and crocodilians).

In conclusion, all these findings together (NCC migration patterns, PNS morphology and its development), support a uniqueness of turtle NCC.

Experimental Procedures

Animals

Turtle embryos (*Trachemys scripta*) were obtained by incubating freshly laid eggs at 28°C as described by Greenbaum (Greenbaum, 2002) until desired stage of development. We followed Cordero & Janzen's staging given that it was more detailed for earlier stages (Cordero and Janzen, 2014). Embryos were collected by gently flushing the inside soft shell with Ringer's solution to detach the embryo from the shell. Embryos were either fixed overnight at 4°C in 4% paraformaldehyde (PFA) or injected with DiI.

Between 2013 and 2019 we obtained close to 60-80 embryos in total from CSUN pond by gathering the gravid females, injecting them with oxytocin so that they will lay eggs in the vivarium, then releasing them back to the pond. These experiments with all the mentioned reptiles have been approved by CSUN IACUC.

Whole mount immunofluorescence

After overnight incubation in blocking buffer (PBS with 1% Triton-X100, 10% goat serum), turtle embryos were incubated with antibodies in PBS overnight at 4°C, then were extensively washed (minimum of 3hrs with at least 6 changes) with PBS and then incubated with secondary antibodies conjugated Alexa Fluor® Dyes 1:500. Next day embryos were washed extensively (minimum of 3hrs with at least 6 changes) in PBS. We also added DAPI to visualize nuclei, 300 nM. Embryos were photographed using a 4x, 10x and 20x lens objectives with a Zeiss A-1 Axiomager and in the instance of Figure 6 images were aligned and positioned next to each other to create the composite wholemount with Photoshop.

Live DiI injection

We used two strategies for these experiments: in the first, early turtle embryos at st.7-9 (Cordero and Janzen, 2014) were collected and injected while still alive with DiI (cell tracker CM-DiI, C-7001, Invitrogen/Molecular Probes) (diluted 1:10 in ethanol in 10% sucrose) inside the neural tube along its length and hindbrain regions. In both strategies we injected DiI with a mouth pipette (~20-50ul) posterior to the hindbrain blowing gently to fill the neural tube all the way through to the tail. These embryos were placed in a Petri dish after rinsing in Ringer solution and incubated with 5ml of DMEM, 10% FBS, penicillin and streptomycin at 37°C for 4-8hrs. We used this higher temperature for the short term

incubation of younger embryos, since we did not get results from longer term at 28°C. The second strategy consisted of culturing the older turtle embryos in the chicken egg white with penicillin and streptomycin at 28°C for longer periods. Most embryos survived after DiI injection (mortality was 25% for 24 hrs). At the end of incubation, the surviving cultured embryos were fixed in 4% PFA for 1 hr to retain morphology, then placed in a vial for overnight fixing at 4°C and kept there until analysis.

Immunofluorescence

Turtle embryos were either mounted in 4% agarose and vibratome sectioned (50 µm sections) and photographed with a Zeiss Axiolmager microscope or were serially dehydrated then cleared in Histosol for paraffin embedding. Paraffin blocks were sectioned (12 µm sections), deparaffinized and serially rehydrated, before rinsing several times in PBS and blocked in 10% normal goat serum for 1 h. Primary antibodies (HNK1 from DSHB or TuJ1 from Covance, see Key Resource Table at the end) were diluted and placed on the slides to incubate overnight at room temperature. Sections were then treated with Alexa Fluor® Dyes fluorescently labelled secondary antibodies diluted 1:500 in PBS. For antibodies details see Key Resource Table.

Acknowledgements

We thank Drs. Meyer Barembaum, Robert Czerny, Cindy Malone and Martin Garcia-Castro for invaluable help in reviewing and helping with the manuscript. We would want to thank the anonymous reviewers at DVDY whose comments improved significantly this manuscript. We also thank Dr. Max Ezin for helpful comments and suggestions during the years that these studies were done. This work was supported by an NIH/NINDS AREA grant 1R15-NS060099-03 MEDB.

References

- Abzhanov A, Tzahor E, Lassar AB, Tabin CJ. 2003 Dissimilar regulation of cell differentiation in mesencephalic (cranial) and sacral (trunk) neural crest cells in vitro. *Development* 130:4567–4579. [PubMed: 12925584]
- Baggiolini A, Varum S, Mateos Jose M, Bettosini D, John N, Bonalli M, Ziegler U, Dimou L, Clevers H, Furrer R, Sommer L. 2015 Premigratory and Migratory Neural Crest Cells Are Multipotent In Vivo. *Cell Stem Cell* 16:314–322. [PubMed: 25748934]
- Baker CV. 2005 *Neural Crest and Cranial Ectodermal Placodes*. New York: Springer, New York pp.67–127 pp.
- Barraud P, Seferiadis AA, Tyson LD, Zwart MF, Szabo-Rogers HL, Ruhrberg C, Liu KJ, Baker CV. 2010 Neural crest origin of olfactory ensheathing glia. *Proc Natl Acad Sci U S A* 107:21040–21045. [PubMed: 21078992]
- Bronner ME, LeDouarin NM. 2012 Development and evolution of the neural crest: an overview. *Dev Biol* 366:2–9. [PubMed: 22230617]
- Cebra-Thomas JA, Betters E, Yin M, Plafkin C, McDow K, Gilbert SF. 2007 Evidence that a late-emerging population of trunk neural crest cells forms the plastron bones in the turtle *Trachemys scripta*. *Evol Dev* 9:267–277. [PubMed: 17501750]
- Cebra-Thomas JA, Terrell A, Branyan K, Shah S, Rice R, Gyi L, Yin M, Hu Y, Mangat G, Simonet J, Betters E, Gilbert SF. 2013 Late-emigrating trunk neural crest cells in turtle embryos generate an osteogenic ectomesenchyme in the plastron. *Dev Dyn* 242:1223–1235. [PubMed: 23904174]
- Chien CB, Piotrowski T. 2002 How the lateral line gets its glia. *Trends Neurosci* 25:544–546. [PubMed: 12392921]
- Clay MR, Halloran MC. 2010 Control of neural crest cell behavior and migration: Insights from live imaging. *Cell Adh Migr* 4:586–594. [PubMed: 20671421]

- Collazo A, Bronner-Fraser M, Fraser SE. 1993 Vital dye labelling of *Xenopus laevis* trunk neural crest reveals multipotency and novel pathways of migration. *Development* 118:363–376. [PubMed: 7693414]
- Cordero G, Janzen FJ. 2014 An enhanced developmental staging table for the painted turtle, *Chrysemys picta* (Testudines: Emydidae). *J Morphol* 275:442–455. [PubMed: 24301536]
- Creuzet S, Couly G, Le Douarin NM. 2005 Patterning the neural crest derivatives during development of the vertebrate head: insights from avian studies. *J Anat* 207:447–459. [PubMed: 16313387]
- Del Barrio MG, Nieto MA. 2004 Relative expression of Slug, RhoB, and HNK-1 in the cranial neural crest of the early chicken embryo. *Dev Dyn* 229:136–139. [PubMed: 14699585]
- Diaz RE, Shylo NA, Roellig D, Bronner M, Trainor PA. 2019 Filling in the phylogenetic gaps: Induction, migration, and differentiation of neural crest cells in a squamate reptile, the veiled chameleon (*Chamaeleo calytratus*). *Developmental Dynamics* 248:709–727. [PubMed: 30980777]
- Dupin E, Creuzet S, Le Douarin NM. 2006 The contribution of the neural crest to the vertebrate body. *Adv Exp Med Biol* 589:96–119. [PubMed: 17076277]
- Dupin E, Ziller C, Le Douarin NM. 1998 The avian embryo as a model in developmental studies: chimeras and in vitro clonal analysis. *Curr Top Dev Biol* 36:1–35. [PubMed: 9342519]
- Eisen JS, Weston JA. 1993 Development of the neural crest in the zebrafish. *Dev Biol* 159:50–59. [PubMed: 8365574]
- Field DJ, Gauthier JA, King BL, Pisani D, Lyson TR, Peterson KJ. 2014 Toward consilience in reptile phylogeny: miRNAs support an archosaur, not lepidosaur, affinity for turtles. *Evolution & Development* 16:189–196. [PubMed: 24798503]
- Gabe M 1970 [Histologic data on the endocrine pancreas of Lepidosaurians (reptiles)]. *Ergeb Anat Entwicklungsgesch* 42:3–61.
- Gilbert SF, Bender G, Betters E, Yin M, Cebra-Thomas JA. 2007 The contribution of neural crest cells to the nuchal bone and plastron of the turtle shell. *Integr Comp Biol* 47:401–408. [PubMed: 21672848]
- Gillis JA, Alsema EC, Criswell KE. 2017 Trunk neural crest origin of dermal denticles in a cartilaginous fish. *Proceedings of the National Academy of Sciences* 114:13200–13205.
- Giovannone D, Ortega B, Reyes M, El-Ghali N, Rabadi M, Sao S, de Bellard ME. 2015 Chicken trunk neural crest migration visualized with HNK1. *Acta Histochem* 117:255–266. [PubMed: 25805416]
- Glenn Northcutt R 2005 The new head hypothesis revisited. *J Exp Zool B Mol Dev Evol* 304:274–297. [PubMed: 16003768]
- Graveson AC, Smith MM, Hall BK. 1997 Neural crest potential for tooth development in a urodele amphibian: developmental and evolutionary significance. *Dev Biol* 188:34–42. [PubMed: 9245509]
- Greenbaum E 2002 A standardized series of embryonic stages for the emydid turtle *Trachemys scripta*. *Canadian Journal of Zoology* 80:1350–1370.
- Hall BK. 2009 *The Neural Crest and Neural Crest Cells in Vertebrate Development and Evolution*. New York: Springer-Verlag,.
- Halloran MC. 2010 Control of neural crest cell behavior and migration. *Cell Adhesion & Migration* 4:586–594. [PubMed: 20671421]
- Horie R, Hazbun A, Chen K, Cao C, Levine M, Horie T. 2018 Shared evolutionary origin of vertebrate neural crest and cranial placodes. *Nature* 560:228–232. [PubMed: 30069052]
- Hou L, Takeuchi T. 1994 Neural crest development in reptilian embryos, studied with monoclonal antibody, HNK-1. *Zoolog Sci* 11:423–431.
- Ido A, Ito K. 2006 Expression of chondrogenic potential of mouse trunk neural crest cells by FGF2 treatment. *Dev Dyn* 235:361–367. [PubMed: 16273527]
- Kague E, Gallagher M, Burke S, Parsons M, Franz-Odenaal T, Fisher S. 2012 Skeletogenic Fate of Zebrafish Cranial and Trunk Neural Crest. *PLOS ONE* 7:e47394. [PubMed: 23155370]
- Kasemeier-Kulesa JC, Kulesa PM, Lefcort F. 2005 Imaging neural crest cell dynamics during formation of dorsal root ganglia and sympathetic ganglia. *Development* 132:235–245. [PubMed: 15590743]

- Kastriti ME, Kameneva P, Kamenev D, Dyachuk V, Furlan A, Hampl M, Memic F, Marklund U, Lallemand F, Hadjab S, Calvo-Enrique L, Ernfors P, Fried K, Adameyko I. 2019 Schwann Cell Precursors Generate the Majority of Chromaffin Cells in Zuckerkandl Organ and Some Sympathetic Neurons in Paraganglia. *Frontiers in Molecular Neuroscience* 12. [PubMed: 30804751]
- Koshiba-Takeuchi K, Mori AD, Kaynak BL, Cebra-Thomas J, Sukonnik T, Georges RO, Latham S, Beck L, Henkelman RM, Black BL, Olson EN, Wade J, Takeuchi JK, Nemer M, Gilbert SF, Bruneau BG. 2009 Reptilian heart development and the molecular basis of cardiac chamber evolution. *Nature* 461:95–98. [PubMed: 19727199]
- Kulesa PM, Fraser SE. 2000 In ovo time-lapse analysis of chick hindbrain neural crest cell migration shows cell interactions during migration to the branchial arches. *Development* 127:1161–1172. [PubMed: 10683170]
- Kulesa PM, Gammill LS. 2010 Neural crest migration: patterns, phases and signals. *Dev Biol* 344:566–568. [PubMed: 20478296]
- Kundrat M 2008 HNK-1 immunoreactivity during early morphogenesis of the head region in a nonmodel vertebrate, crocodile embryo. *Naturwissenschaften* 95:1063–1072. [PubMed: 18668221]
- Kuratani S, Kusakabe R, Hirasawa T. 2018 The neural crest and evolution of the head/trunk interface in vertebrates. *Developmental Biology* 444:S60–S66. [PubMed: 29408469]
- Le Douarin NM, Dupin E. 2018 The “beginnings” of the neural crest. *Developmental Biology*.
- Le Douarin NM, Teillet MA. 1973 The migration of neural crest cells to the wall of the digestive tract in avian embryo. *J Embryol Exp Morphol* 30:31–48. [PubMed: 4729950]
- Levi-Montalcini R, Booker B. 1960 Destruction of the sympathetic ganglia in mammals by an antiserum to a nerve-growth protein. *Proceedings of the National Academy of Sciences* 46:384.
- Loring JF, Erickson CA. 1987 Neural crest cell migratory pathways in the trunk of the chick embryo. *Dev Biol* 121:220–236. [PubMed: 3552788]
- McGonnell IM, Graham A. 2002 Trunk neural crest has skeletogenic potential. *Curr Biol* 12:767–771. [PubMed: 12007423]
- McLennan R, Bailey CM, Schumacher LJ, Teddy JM, Morrison JA, Kasemeier-Kulesa JC, Wolfe LA, Gogol MM, Baker RE, Maini PK, Kulesa PM. 2017 DAN (NBL1) promotes collective neural crest migration by restraining uncontrolled invasion. *The Journal of Cell Biology* 216:3339. [PubMed: 28811280]
- Replogle MR, Sreevidya VS, Lee VM, Laiosa MD, Svoboda KR, Udvadia AJ. 2018 Establishment of a murine culture system for modeling the temporal progression of cranial and trunk neural crest cell differentiation. *Disease Models & Mechanisms* 11:dmm035097. [PubMed: 30409814]
- Reyes M, Zandberg K, Desmawati I, de Bellard ME. 2010 Emergence and migration of trunk neural crest cells in a snake, the California Kingsnake (*Lampropeltis getula californica*). *BMC Dev Biol* 10:52. [PubMed: 20482793]
- Rice R, Cebra-Thomas J, Haugas M, Partanen J, Rice DPC, Gilbert SF. 2017 Melanoblast development coincides with the late emerging cells from the dorsal neural tube in turtle *Trachemys scripta*. *Sci Rep* 7:12063. [PubMed: 28935865]
- Rice R, Kallonen A, Cebra-Thomas J, Gilbert SF. 2016 Development of the turtle plastron, the order-defining skeletal structure. *Proc Natl Acad Sci U S A* 113:5317–5322. [PubMed: 27114549]
- Richardson J, Gauert A, Briones Montecinos L, Fanlo L, Alhashem Zainalabdeen M, Assar R, Marti E, Kabla A, Hartel S, Linker C. 2016 Leader Cells Define Directionality of Trunk, but Not Cranial, Neural Crest Cell Migration. *Cell Reports* 15:2076–2088. [PubMed: 27210753]
- Rogers CD, Jayasena CS, Nie S, Bronner ME. 2012 Neural crest specification: tissues, signals, and transcription factors. *Wiley Interdiscip Rev Dev Biol* 1:52–68. [PubMed: 23801667]
- Rupik W 2002 Early development of the adrenal glands in the grass snake *Natrix natrix* L. (Lepidosauria, Serpentes). *Adv Anat Embryol Cell Biol* 164:I–XI, 1–102. [PubMed: 12080925]
- Sadaghiani B, Vielkind JR. 1990 Distribution and migration pathways of HNK-1-immunoreactive neural crest cells in teleost fish embryos. *Development* 110:197–209. [PubMed: 1706978]
- Santagati F, Rijli FM. 2003 Cranial neural crest and the building of the vertebrate head. *Nat Rev Neurosci* 4:806–818. [PubMed: 14523380]

- Schumacher LJ, Kulesa PM, McLennan R, Baker RE, Maini PK. 2016 Multidisciplinary approaches to understanding collective cell migration in developmental biology. *Open Biol* 6.
- Schwarz Q, Maden CH, Davidson K, Ruhrberg C. 2009 Neuropilin-mediated neural crest cell guidance is essential to organise sensory neurons into segmented dorsal root ganglia. *Development* 136:1785–1789. [PubMed: 19386662]
- Serbedzija GN, Bronner-Fraser M, Fraser SE. 1989 A vital dye analysis of the timing and pathways of avian trunk neural crest cell migration. *Development* 106:809–816. [PubMed: 2562671]
- Serbedzija GN, Bronner-Fraser M, Fraser SE. 1992 Vital dye analysis of cranial neural crest cell migration in the mouse embryo. *Development* 116:297–307. [PubMed: 1283734]
- Shen X-X, Liang D, Wen J-Z, Zhang P. 2011 Multiple Genome Alignments Facilitate Development of NPCL Markers: A Case Study of Tetrapod Phylogeny Focusing on the Position of Turtles. *Molecular Biology and Evolution* 28:3237–3252. [PubMed: 21680872]
- Simkin JE, Zhang D, Stamp LA, Newgreen DF. 2019 Fine scale differences within the vagal neural crest for enteric nervous system formation. *Developmental Biology* 446:22–33. [PubMed: 30448439]
- Smith M, Hickman A, Amanzee D, Lumsden A, Thorogood P. 1994 Trunk neural crest origin of caudal fin mesenchyme in the zebrafish *Danio rerio*. *Proc R Soc Lond B Biol Sci* 256:137–145.
- Szabo A, Melchionda M, Nastasi G, Woods ML, Campo S, Perris R, Mayor R. 2016 In vivo confinement promotes collective migration of neural crest cells. *The Journal of Cell Biology* 213:543. [PubMed: 27241911]
- Theveneau E, Mayor R. 2012 Neural crest migration: interplay between chemorepellents, chemoattractants, contact inhibition, epithelial-mesenchymal transition, and collective cell migration. *Wiley Interdisciplinary Reviews: Developmental Biology* 1:435–445. [PubMed: 23801492]
- Tokita M, Kuratani S. 2001 Normal Embryonic Stages of the Chinese Softshelled Turtle *Pelodiscus sinensis* (Trionychidae). *Zoological Science* 18:705–715.
- Trainor PA. 2005 Specification of neural crest cell formation and migration in mouse embryos. *Semin Cell Dev Biol* 16:683–693. [PubMed: 16043371]
- Trentin A, Glavieux-Pardanaud C, Le Douarin NM, Dupin E. 2004 Self-renewal capacity is a widespread property of various types of neural crest precursor cells. *Proceedings of the National Academy of Sciences of the United States of America* 101:4495–4500. [PubMed: 15070746]
- Tzika AC, Helaers R, Schramm G, Milinkovitch MC. 2011 Reptilian-transcriptome v1.0, a glimpse in the brain transcriptome of five divergent Sauropsida lineages and the phylogenetic position of turtles. *EvoDevo* 2:19. [PubMed: 21943375]
- Vega-Lopez GA, Cerrizuela S, Aybar MJ. 2017 Trunk neural crest cells: formation, migration and beyond. *Int J Dev Biol* 61:5–15. [PubMed: 28287247]
- Williston SW, Gregory WK. 1925 *The osteology of the reptiles* Cambridge, : Harvard University Press xiii, 300 p. pp.

Key findings:

- Turtle trunk neural crest migration follows unique patterns.
- Pharyngula trunk NCC may contribute to turtle plastron.
- Turtle PNS nerves are larger than other squamates.

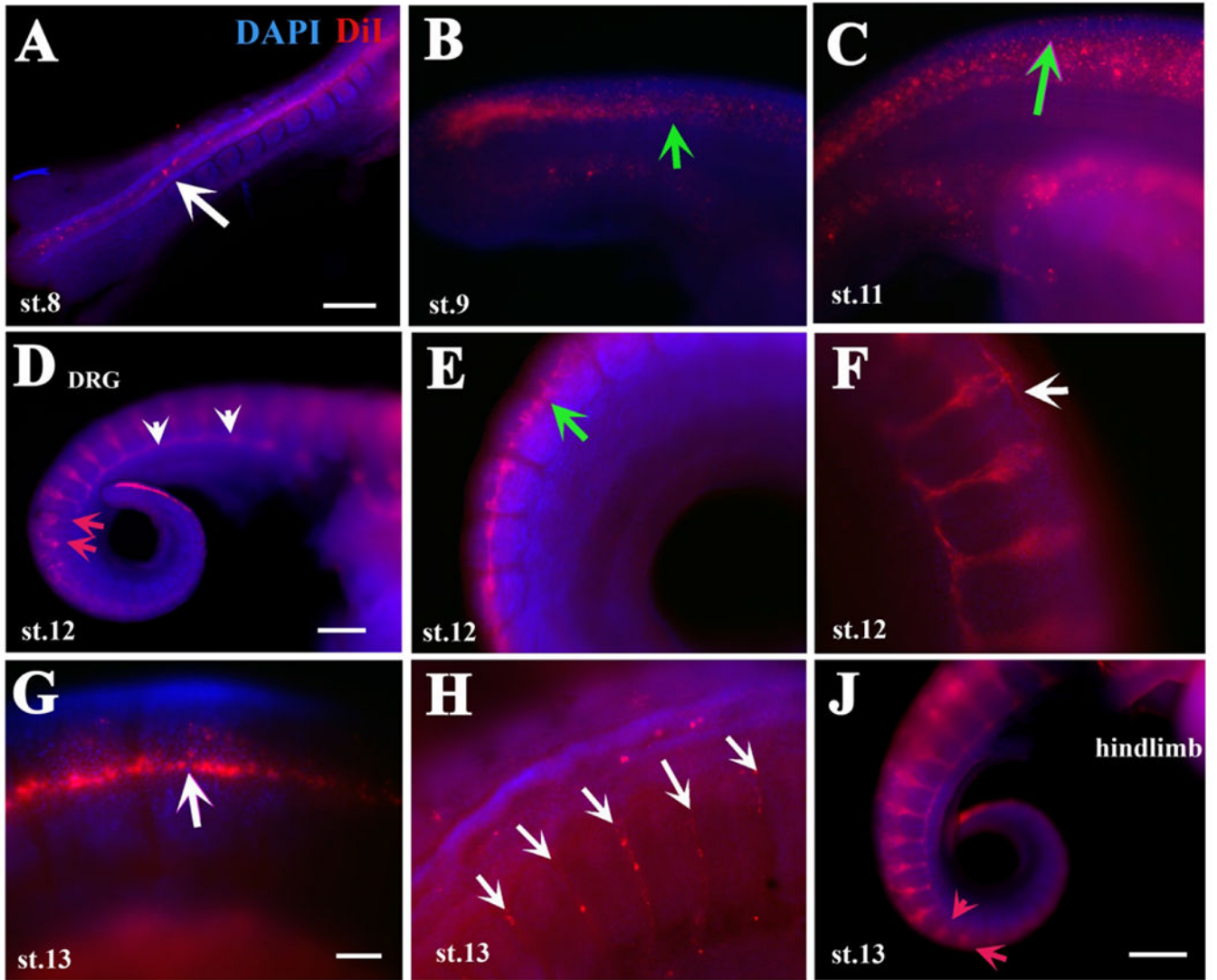


Figure 1.

DiI labels turtle neural crest cells migration in detail.

Turtle embryos at different stages of development (identified in each frame as “st.xx”) were injected with DiI inside their NT and incubated overnight at 28°C. A shows a stage 8 embryo with DiI cells in NT. Arrow in A points to delaminated NCC. B, C shows a stage 9 or 11 embryo respectively, with delaminated DiI cells on top of NT. Green arrows in B, C point to scattered, delaminated tNCC. D-F shows 2 stage 12 embryos, D and E are from same embryo. Red arrows in D point to tNCC migrating NCC in rostral portion of somites, white arrowheads point to sympathetic chain. Green arrow in E points to recently delaminated and dispersed tNCC. G shows a line of DiI cells along anterior to posterior axis. White arrows in F, G point to a line of DiI cells along NT. H image is at hindlimb levels and arrows point to DiI-positive cells migrating inter-somatically. Red arrows in J point to tNCC entering medial portion of the somites. Rostral is to the left caudal to the right of the images. DAPI in blue. Scale bar corresponds to 100µm.

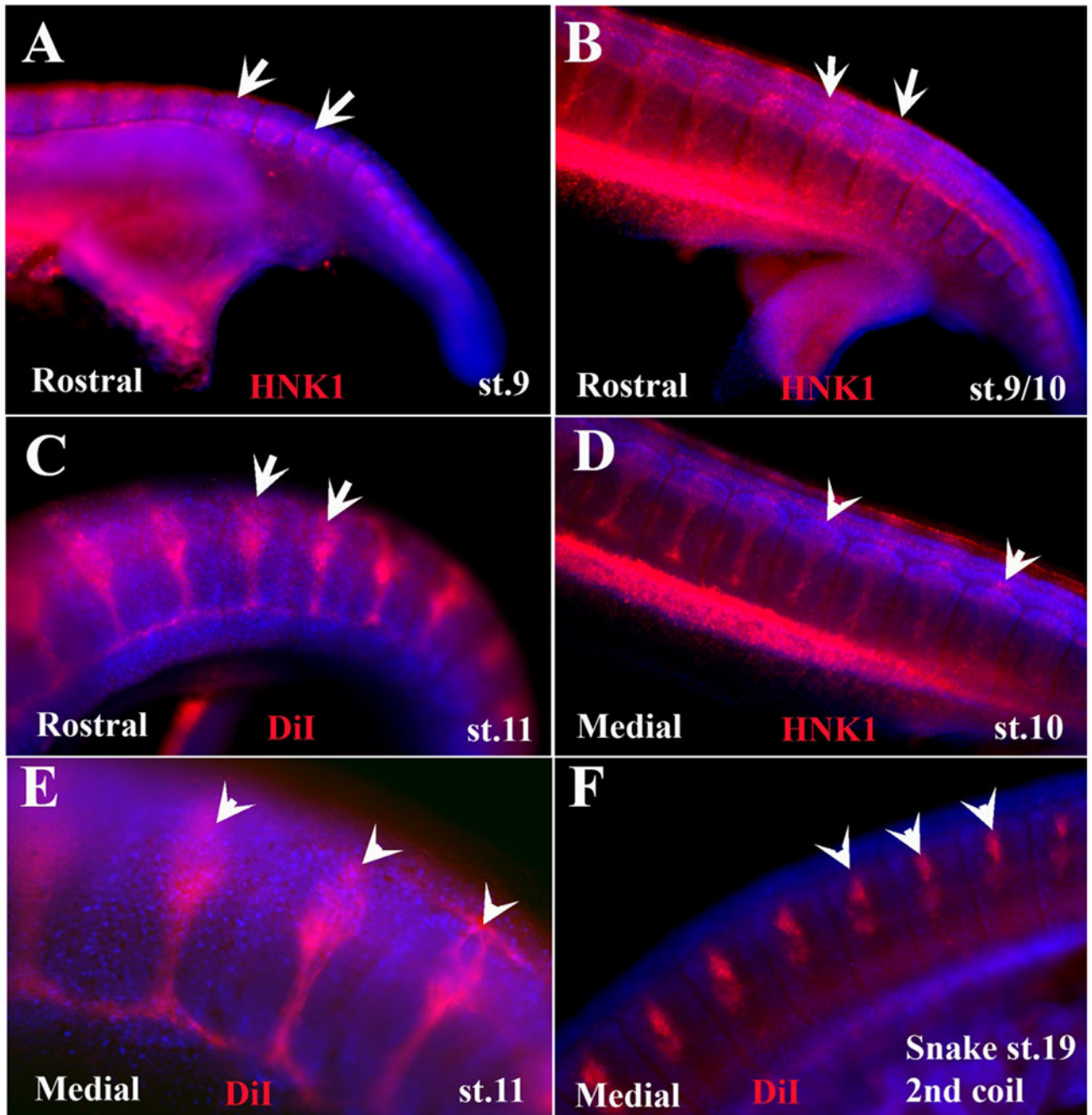


Figure 2.
 Wholemount embryos showing varied segmental migration. Turtle and one snake embryos at different stages of development were labeled with HNK1 (red) or DiI. On the bottom left of each image is either “Rostral” or “Medial” for tNCC migration. The images have had their contrast increased in order to make the somite area (labeled in blue with DAPI) and tNCC. Each of the embryo stages is listed. Scale bar corresponds to 100 μ m.

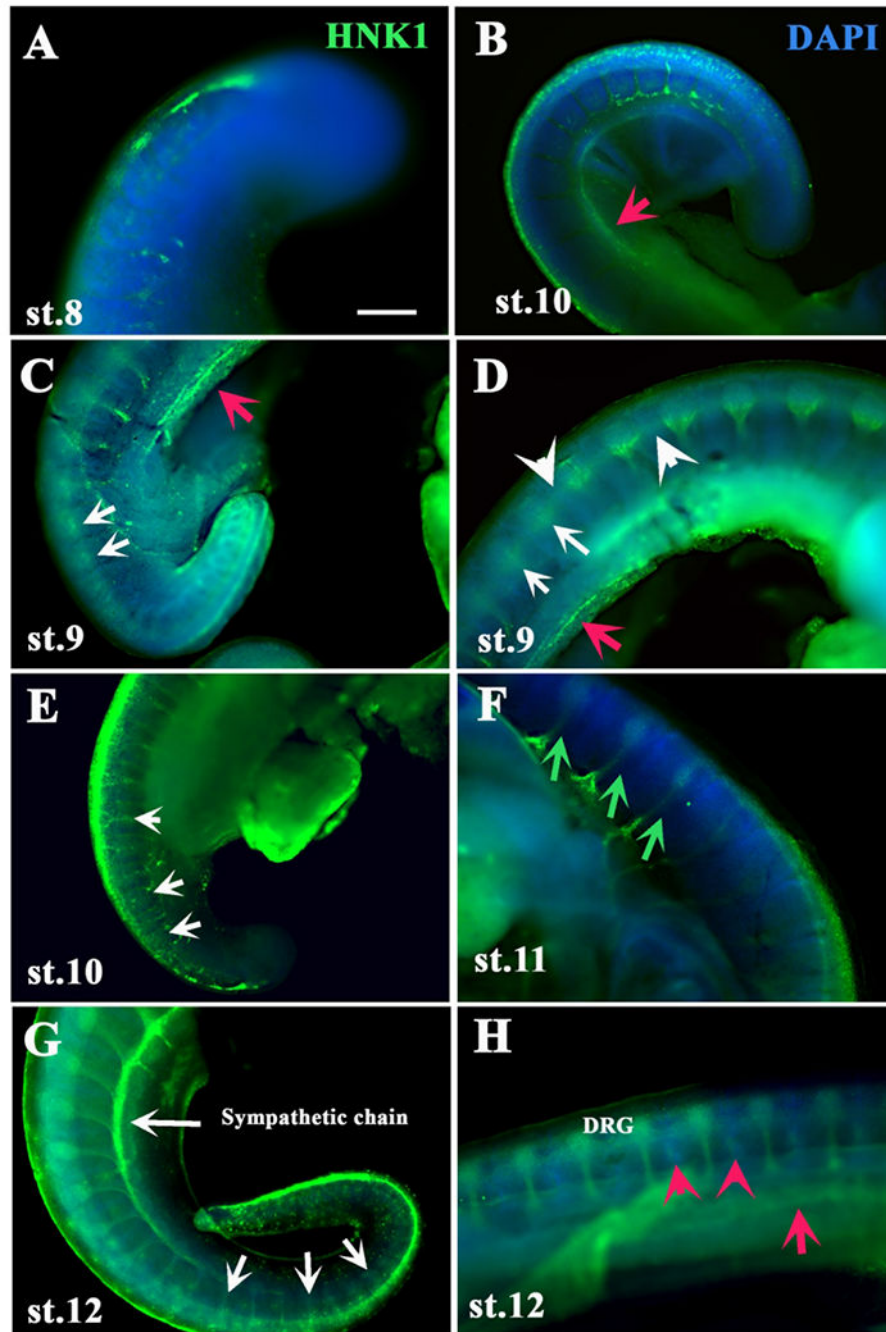


Figure 3.
 HNK1 labels turtle neural crest cells migration in detail.
 Turtle embryos at different stages of development (identified in each frame as “st.xx”) were labeled with HNK1 (green). A, B shows tail ends from a st.8 & 9 embryos with HNK1 cells beginning to delaminate from NT. C, D shows a st.9 with delaminated tNCC cells migrating segmentally. E shows st.10 embryo with HNK1 cells migrating medially through the somites (white arrows). F is a st.11 embryo showing spinal nerves labeled with HNK1 (green arrows). G, H shows two st.12 embryos stained with HNK1, labeling the sympathetic chain and

tNCC migrating between DRG (red arrowheads). Red arrows point to HNK1 cells along mesodermal line. White arrows point to segmental migration of tNCC. White arrowheads point to line of HNK1 along trunk in D. Red arrowheads point to HNK1 tNCC migrating between somites. DAPI in blue. Scale bar corresponds to 100 μ m for all images

Author Manuscript

Author Manuscript

Author Manuscript

Author Manuscript

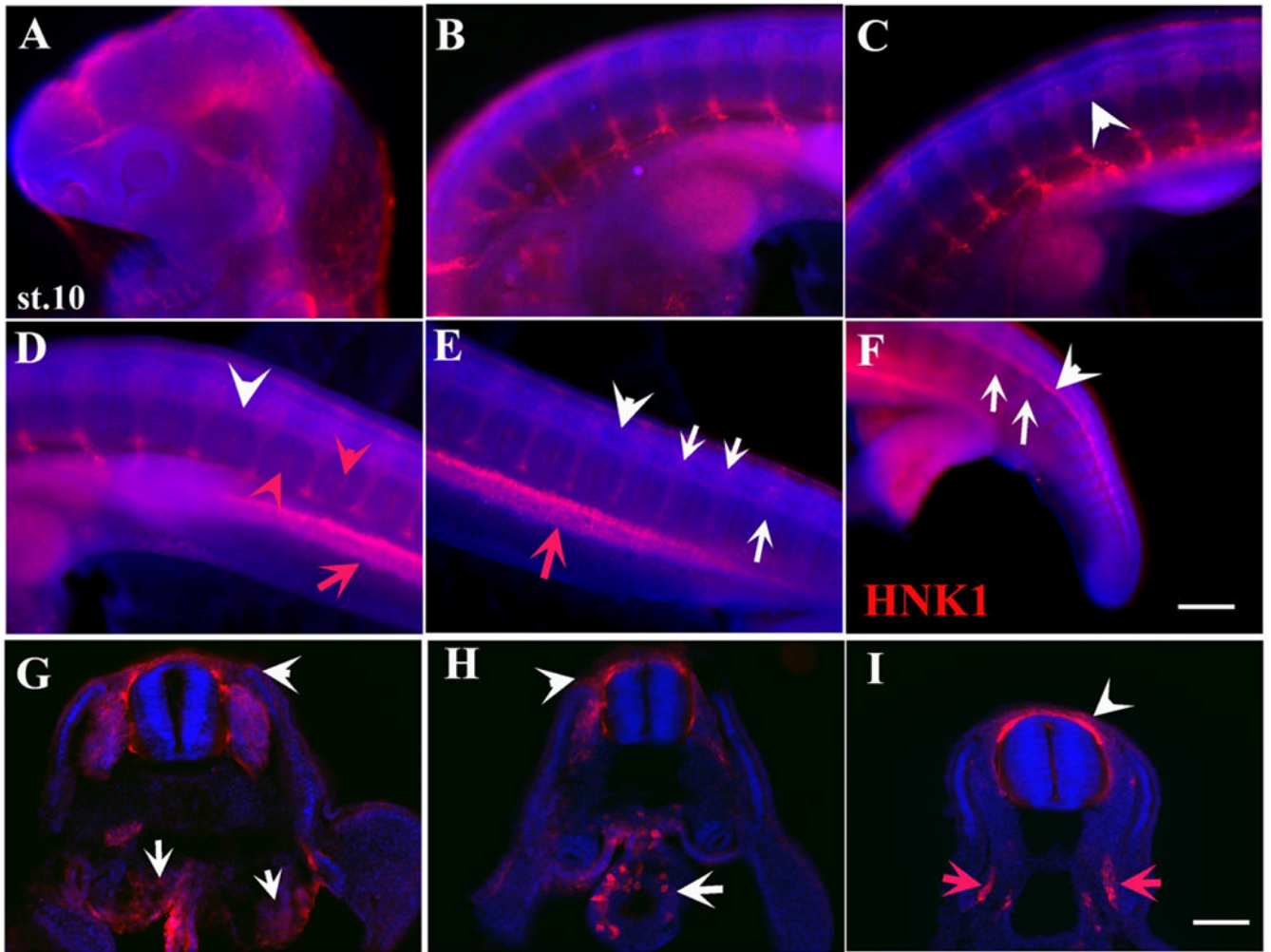


Figure 4.

HNK1 labels turtle neural crest cell migration in great detail.

A stage 10 embryo wholemount with HNK1 (red) and DAPI (blue). A-F shows a trunk to tail set of images of the embryo. White arrowheads in C-F point to tNCC migrating as a line along NT. Red arrows point to laterally migrating cells between limb buds (D-E). Red arrowheads point to HNK1 cells migrating between DRG (D-E). White arrows point to tNCC migrating segmentally (E-F). G-I are sections throughout this embryo. White arrow in G shows large number of HNK1 cells in mesonephros, while white arrowhead to cells under ectoderm. White arrow in H shows HNK1 cells inside the gut. More caudal section in I shows NCC migrating in larger numbers outside and dorsal to NT (white arrowhead). Red arrows in I show tNCC migrating in lateral mesoderm. Scale bar corresponds to 100 μ m.

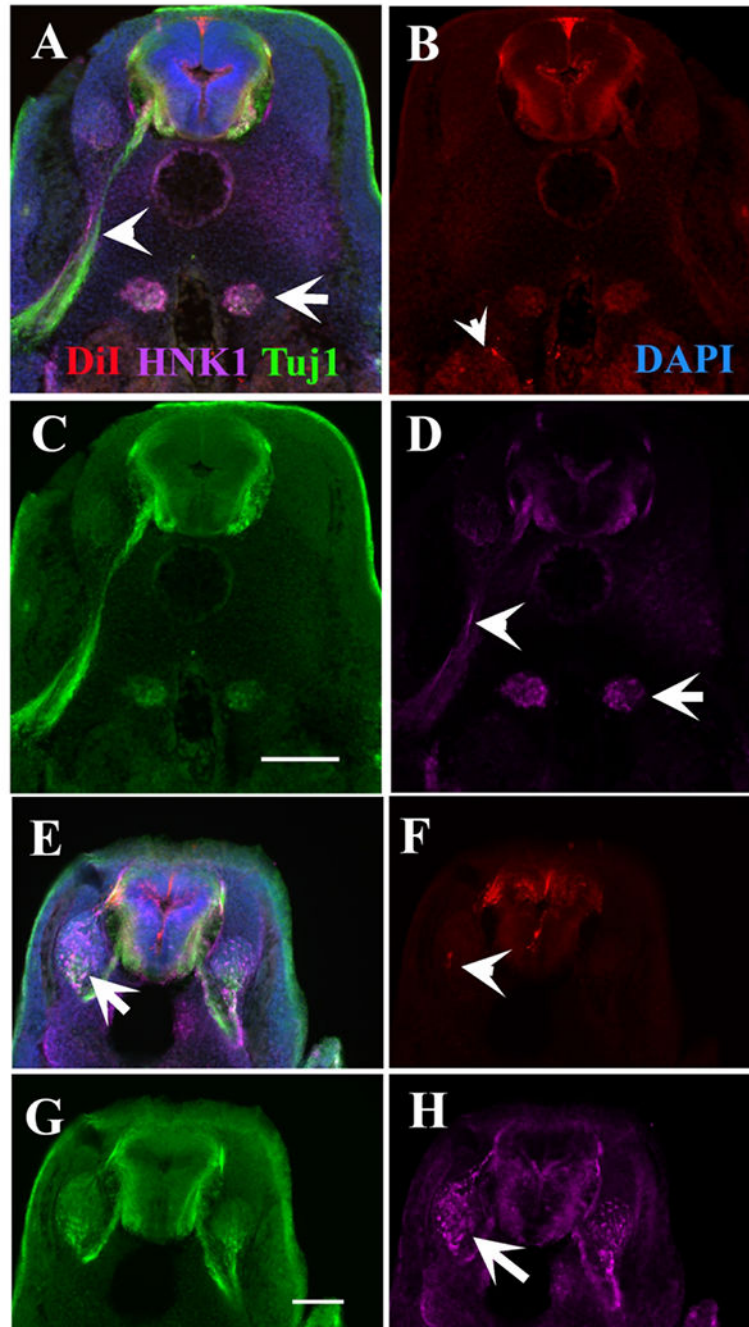


Figure 5.

HNK1 and TuJ1 label different cells in DiI turtle embryo.

A stage 11 turtle embryo double stained with HNK1 (magenta) and TUJ1 (green) after DiI labeling. A is the triple labeled section, with B-D showing each separate antibody or DiI labeling. Arrowheads point to spinal nerve, and arrow to condensing sympathetic ganglia. E is the triple labeled section, with F-H showing each separate antibody or DiI labeling. Arrow points to the condensing DRG with many HNK1-positive cells, and arrowhead to scattered DiI labeled cells in DRG in F. Scale bar corresponds to 100 μ m.

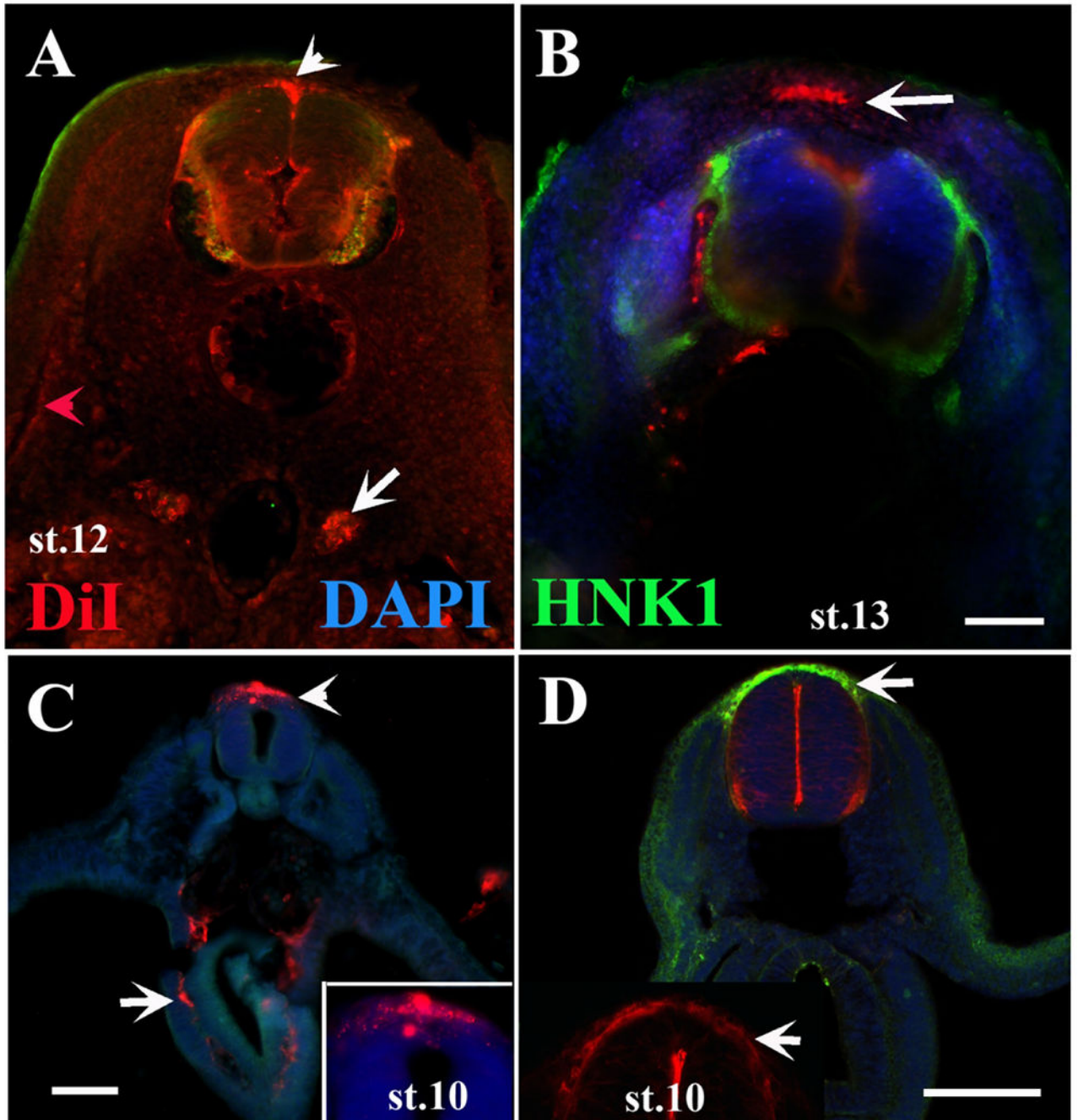


Figure 6.

Sections through DiI turtle.

Turtle embryos at different stages of development were injected with DiI inside their NT, incubated at 28°C and stained with HNK1 (green). A is a st.12 embryo section between limbs, arrows show migrating DiI cells deeper than ectoderm (red arrowhead) and by the dorsal aorta (arrow). B, section through an older embryo (st.13) shows DiI cells over the NT (arrow) as well as next to NT. C, midtrunk of a st.10 embryo showing delaminated DiI NCC (arrowhead) and cells inside the developing gut (arrow). D are mid-trunk sections. Arrows

points to delaminated DiI/HNK1 NCC. Inset in D is a magnification of neural tube section, white arrows pointing to delaminated tNCC. Scale bar corresponds to 100 μ m.

Author Manuscript

Author Manuscript

Author Manuscript

Author Manuscript

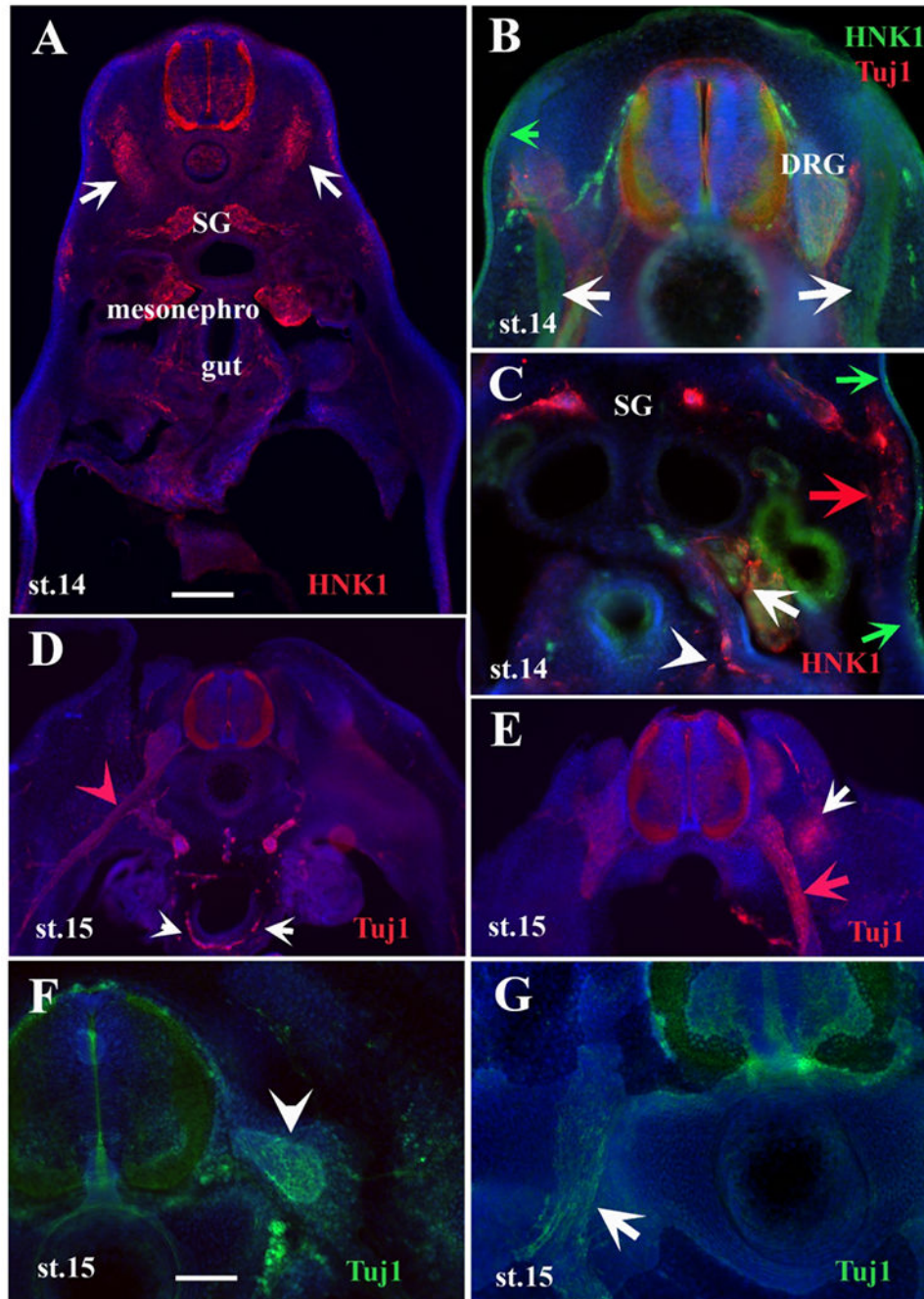


Figure 7.

TuJ1 and HNK1 labels turtle developing peripheral nervous system.

Migrating TNCC and developing PNS cells are labeled with HNK1 or TuJ1 in turtle embryo sections at different stages. A-E are sections at different axial levels between fore and hindlimb of st.14 embryos. F-G of st.15 embryo posterior to forelimb. A is a section before hindlimb. Arrows point to HNK1+ cells condensed in ventromedial mesoderm. B is a section above forelimb, with HNK1 (white arrows) cluster of HNK1+ cells. Green arrow points to slightly HNK1-positive ectoderm. C is a mid-trunk section showing enteric cells

positive for HNK1 (white arrowhead), HNK1 cells in mesonephroi (white arrow), HNK1 migrating cells through mesoderm (red arrow), and slightly HNK1-positive ectoderm (green arrows). D is a section past hindlimb, white arrowheads point to enteric cells positive for TuJ1, red arrowhead to spinal nerve. E is a section rostral to hindlimb, white arrow points to TuJ1 positive cells next to spinal nerve. Notice the large spinal nerve in D and E (red arrow). White arrowhead in F point to DRG, and white arrow in G point to spinal nerve labeled with TuJ1. Scale bar corresponds to 100 μ m. Nuclei are labeled with DAPI in blue. SG: sympathetic ganglion.

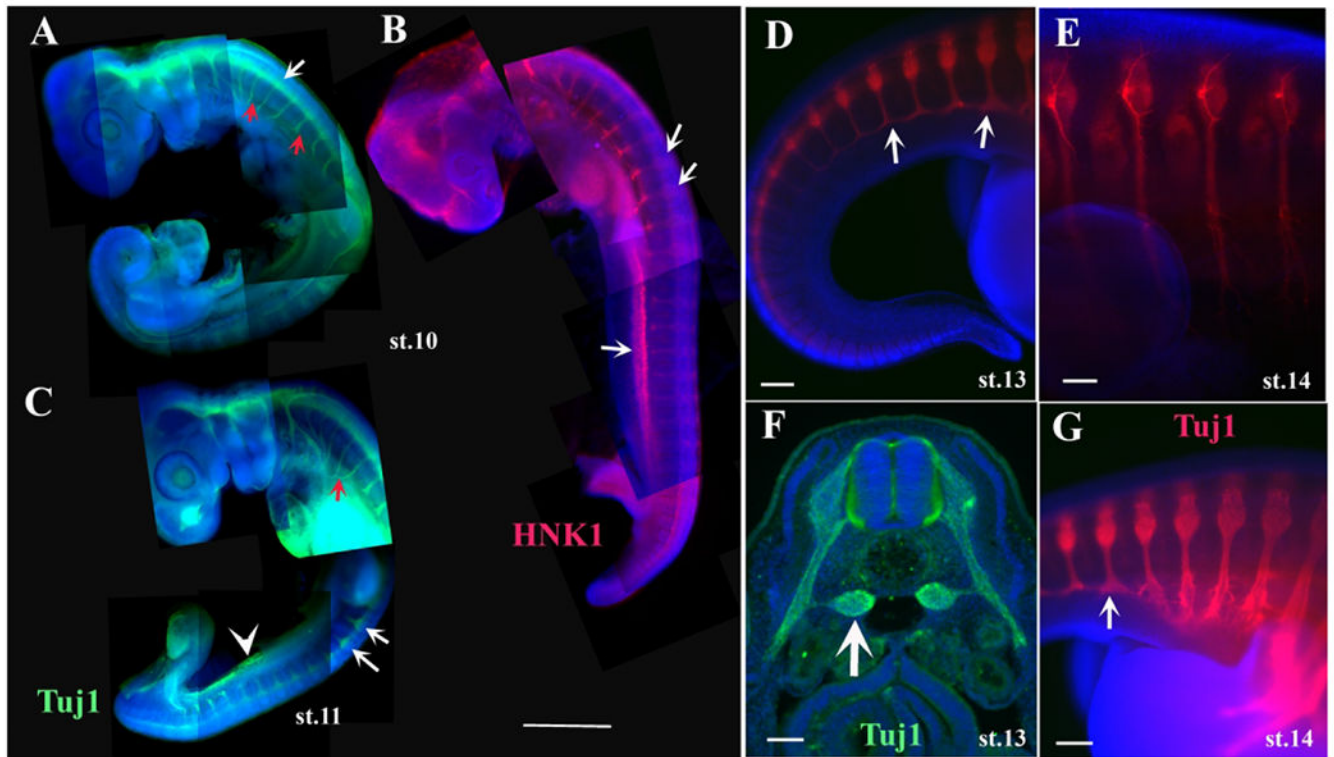


Figure 8.

Tuj1 and HNK1 labels turtle developing peripheral nervous system.

Turtle embryos at stage 10 (A, B) and 11 (C) stained with Tuj1 (green) or HNK1 (red).

White arrows in A, B and C point to tNCC cells in DRG. Red arrows in A point to the PNS

nerves. Turtle embryos at stage 13 or 14 at tail end (D, G) and forelimb (E) were

wholemout stained with Tuj1. White arrows in D, F point to sympathetic ganglia. Scale bar

corresponds to 500 μ m in A-C. Scale bar corresponds to 100 μ m in D-E, G. Scale bar

corresponds to 50 μ m in F.

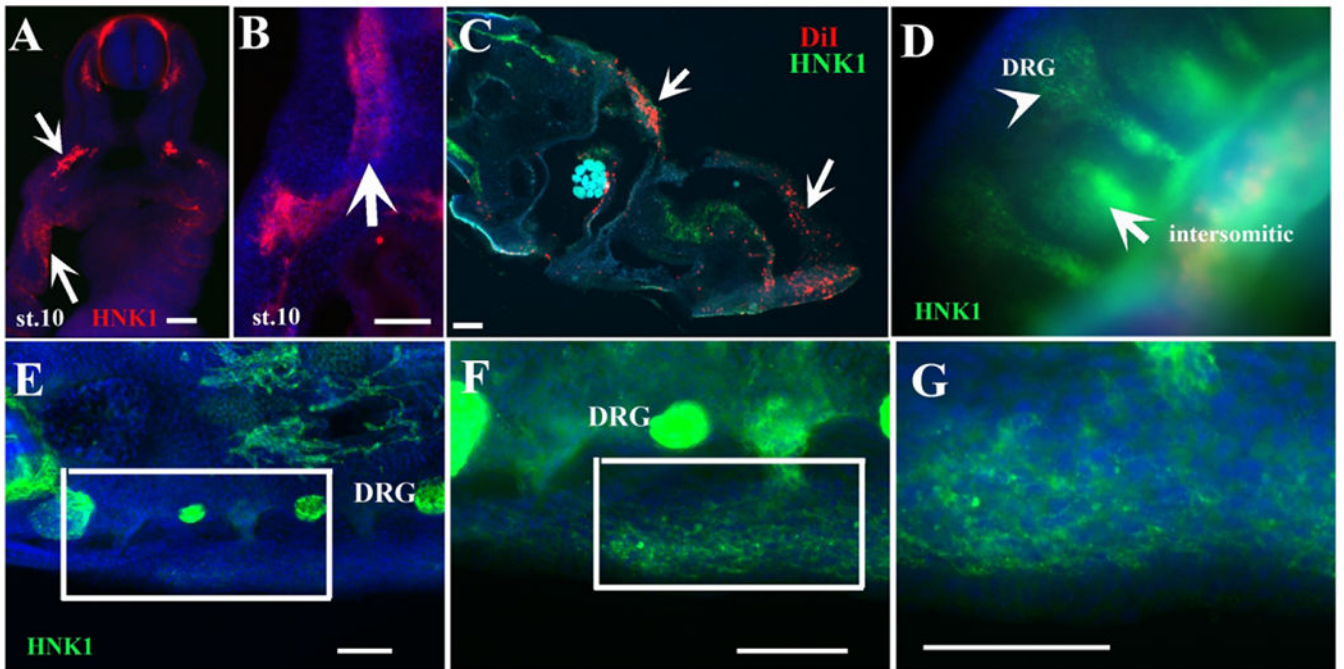


Figure 9.

Turtle NCC along carapace and plastron pathways.

A-B show sections in turtle embryos labeled with HNK1 (red). Arrows in A and B points to HNK1-labeled tNCC migrating ventrally through the mesodermal flank. C, section through a DiI injected st.9 embryo. White arrows point to DiI cells with few scattered HNK1 positive cells in green in the mesoderm. Arrow in D points to intersomitic HNK1 cells (green) in a transverse section spanning trunk region between limbs and migrating along the lateral mesoderm, arrowhead points to DRG. D-G show a wholemount (D) or sections through the midtrunk of a st.12 embryo stained with HNK1 (green). Inset in E is magnified in F. Inset in F is magnified in G, corresponding to line of NCCs in lateral plate mesoderm s. Scale bar corresponds to 100μm.

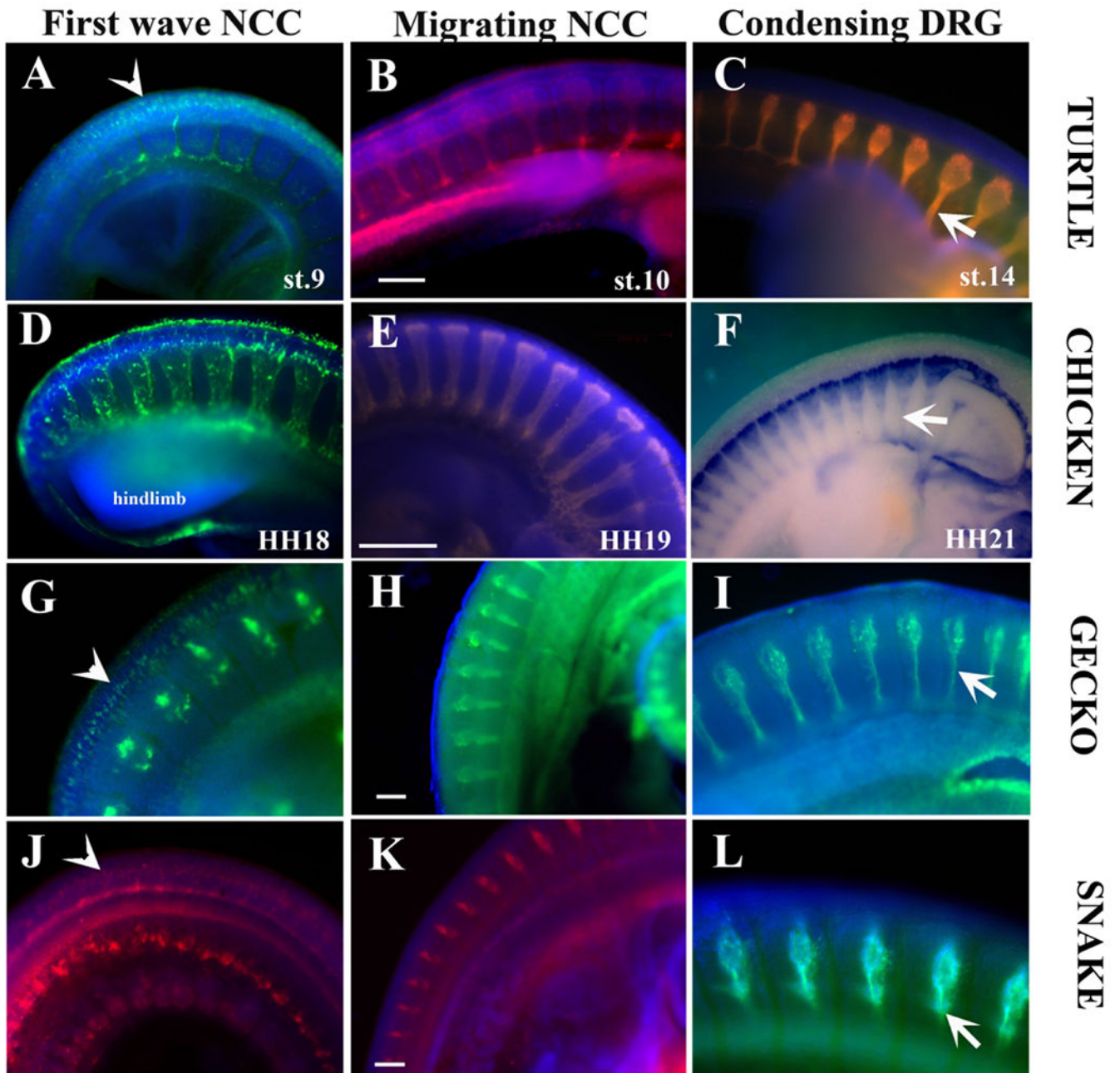


Figure 10.

Peripheral Nervous System development comparison across reptiles.

We generated a comparison across sauropsids of peripheral nervous system development. A-C corresponds to turtle (*Trachemys scripta*). D-F to chicken (*Gallus gallus*). G-I to Gecko (*Gecko gecko*). J-L to snake (*Lampropeltis californiae*). All samples shown are wholemount labeled with HNK1, except for F which shows Sox10 in situ. A, D, G and J show early delaminated tNCC labeled with HNK1. B, E, H and K show tNCC at peak of migration. C, F, I and L show condensing DRGs in these embryos. Scale bar corresponds to 100 μ m.

KEY RESOURCES TABLE

REAGENT or RESOURCE	SOURCE	IDENTIFIER
Antibodies		
Mouse HNK-1 IgM	DSHB	Cat#3H5
Rabbit anti-FoxD3	David Raible	
TuJ1 clone	COVANCE	TUJ1
Alexa 488 anti-mouse IgM	Invitrogen	Cat# A-21042
Alexa 488 anti-rabbit IgG	ThermoFisher	Cat#A-11034
Alexa 594 anti-rabbit IgG	ThermoFisher	Cat#A 11037
Alexa 647 anti-mouse IgM	ThermoFisher	Cat#A-21238
cell tracker CM-DiI	Invitrogen	Cat# C-7001
DAPI	Molecular Probes	
Biological Samples		
Chemicals, Peptides, and Recombinant Proteins		
BSA	ThermoFisher	Cat#BP-1600-100
Permafluor	ThermoFisher	TA-006-FM
Experimental Models: Organisms/Strains		
Red slider turtle (<i>Trachemys scripta</i>)	CSUN pond/Vivarium	
Chicken embryos (<i>Gallus gallus</i>)	AA Laboratories, Westminster, CA	
California Kingsnake (<i>Lampropeltis getula californiae</i>)	CSUN Vivarium	
Tokay gecko (<i>Gekko gecko</i>)	Indonesia market	
Plasmid for RNA		
ckSox1O	Marianne Bronner	
Software and Algorithms		
Excel	Microsoft	https://products.office.com/en-us/excel
AxioVision Rel. 4.8	Zeiss	https://www.zeiss.com/microscopy/int/downloads/axiovision-downloads.html